Chapter 2

CryoEM Analysis of Capsid Assembly and Structural Changes Upon Interactions with a Host Restriction Factor, TRIM5α

Gongpu Zhao and Peijun Zhang

Abstract

After virus fusion with a target cell, the viral core is released into the host cell cytoplasm and undergoes a controlled disassembly process, termed uncoating, before or as reverse transcription takes place. The cellular protein TRIM5α is a host cell restriction factor that blocks HIV-1 infection in rhesus macaque cells by targeting the viral capsid and inducing premature uncoating. The molecular mechanism of the interaction between capsid and TRIM5α remains unclear. Here, we describe an approach that utilizes cryo-electron microscopy (cryoEM) to examine the structural changes exerted on HIV-1 capsid (CA) assembly by TRIM5α binding. The TRIM5α interaction sites on CA assembly were further dissected by combining cryoEM with pair-wise cysteine mutations that crosslink CA either within a CA hexamer or between CA hexamers. Based on the structural information from cryoEM and crosslinking results from in vitro CA assemblies and purified intact HIV-1 cores, we demonstrate that direct binding of TRIM5α CC-SPRY domains to the viral capsid results in disruption and fragmentation of the surface lattice of HIV-1 capsid, specifically at inter-hexamer interfaces. The method described here can be easily adopted to study other important interactions in multi-protein complexes.

Key words CryoEM, Uncoating, HIV-1 restriction factor, TRIM5α, HIV-1 Capsid

1 Introduction

The mature type 1 human immunodeficiency virus (HIV-1), the agent responsible for acquired immunodeficiency syndrome (AIDS), contains a conical capsid that encloses the RNA viral genome. The HIV-1 capsid comprises ~1,500 copies of capsid protein (CA) subunits which assemble into a fullerene cone-shaped structure [1]. HIV-1 CA consists of an N-terminal domain (NTD) and a C-terminal domain (CTD) connected by a flexible linker. A number of atomic structures of individual CA domains as well as full-length protein have been solved [2–12]. Due to its unprecedented polymorphism and asymmetric architecture, it is difficult to determine the structure of the native HIV-1 viral core.

Elisa Vicenzi and Guido Poli (eds.), *Human Retroviruses: Methods and Protocols*, Methods in Molecular Biology, vol. 1087,
DOI 10.1007/978-1-62703-670-2_2,

Several alternative approaches have been employed to shed light on the structure of HIV-1 capsid, including cryo-electron microscopy (cryoEM) of helical assemblies and two-dimensional arrays [13, 14]. Most recently, atomic models of the basic building blocks of the fullerene cone, CA pentamers and CA hexamers, were determined by the Yeager group using an elegant crosslinking strategy for X-ray crystallography [15–17]. Recombinant full-length CA spontaneously assembles into helical tubes under high salt conditions [1], and the structure of these closely resembles authentic viral core. A pseudo-atomic model of helically assembled CA was recently constructed based on the cryoEM structure of in vitro assembled tubes [10]. In addition to previously identified NTD–NTD, NTD–CTD, and CTD dimer interactions [7, 13, 14] that are involved in capsid assembly, this CA assembly structure revealed a novel CTD–CTD trimer interface at the local threefold axis of the CA lattice, which plays important roles in uncoating and capsid stability [10]. Taken together, these structural findings have provided a firm foundation for the study of retroviral capsid function, including uncoating and interaction with host cell factors.

HIV-1 capsid uncoating is a very important, yet obscure, early post-entry event. Recent studies have suggested that uncoating is a tightly controlled process: uncoating too early or too late impairs viral infectivity [18, 19]. Because of its critical role during HIV-1 replication, capsid is a target of a host restriction factor, Trim5 [20–23]. TRIM5 plays an important role in the innate immune defense against retroviruses, including HIV-1 [21, 24–27]. The α splice variant of TRIM5 in rhesus macaque cells blocks HIV-1 after viral entry and before reverse transcription [21]. Several studies suggest that TRIM5α interacts with viral capsids and induces premature capsid uncoating [28–31]. Very recently, TRIM5 was identified to have double duty in HIV-1 restriction. Other than inducing premature uncoating, TRIM5 is also involved in activating a cellular innate immune response by acting as a pattern recognition receptor for retrovirus capsid [32]. TRIM5α is a member of a tripartite motif (TRIM) family of proteins, which contain RING, B-box 2, and coiled-coil (RBCC) domains. TRIM5α also has a C-terminal B30.2/SPRY domain [33–35]. All four domains have distinctive functions and contribute collectively to the antiviral function of TRIM5α. The RING domain is an E3 ubiquitin ligase [36, 37] and its self-ubiquitylation correlates to HIV-1 restriction [38]. While the CC domain is necessary and sufficient for TRIM5α homo-dimerization [25, 39–41], the B-box 2 domain is essential for higher-order association among TRIM5α dimers and TRIM5α binding avidity to capsid [42, 43]. The C-terminal B30.2/SPRY domain binds to viral capsid and determines the specificity of restriction [25, 26, 31, 44–48]. In vitro, specific recognition and binding to a hexagonal CA lattice requires both the CC and SPRY domains [40]. Full-length chimera TRIM5-21R can

spontaneously self-assemble into a hexagonal lattice that is complementary to the CA lattice [49]. Our recent study also shows that, at high concentration, TRIM5α CC-SPRY alone can bind the HIV-1 capsid assembly and disrupt the assembly lattices [50].

In this chapter, we describe, in detail, our protocols to examine the interaction between TRIM5α and CA assembly by cryoEM. Based on the structural models derived from cryoEM and X-ray crystallography, we designed pair-wise cysteine mutations and chemical crosslinking that distinguish the inter- and the intra-hexamer interactions to probe which CA interface is affected by TRIM5α interaction.

2 Materials

2.1 Equipment

1. FPLC system: AKTA Explorer with Unicorn software, 5 ml Hi-Trap QP column and 5 ml Hi-Trap SP column, and Hi-Load Superdex 75 26/60 column (GE Healthcare, Piscataway, NJ).
2. Vertical electrophoresis system: XCell SureLock Mini-Cell (Invitrogen, Carlsbad, CA).
3. Glow-discharge device model 100× (EMS, Hatfield, PA).
4. FEI transmission electron microscopes (FEI Corp., OR): Tecnai T12 with LaB_6 filament, a single-tilt room-temperature specimen holder and a Gatan 2K×2K CCD camera; Tecnai TF20 microscope with a Field Emission Gun, equipped with a Gatan 4K×4K CCD camera.
5. Plunge-freezing devices: Vitrobot Mark III Automated Plunger (FEI Corp., OR) or home-made MRC-type gravity plunger.

2.2 Reagents

1. The cDNA encoding gag polyprotein, $pr55^{gag}$ can be obtained from the NIH AIDS Research and Reference Reagent Program, Division of AIDS, NIAID, NIH [51].
2. pET21 and Rosetta 2 (DE3) (EMD chemicals, Inc. San Diego, CA).
3. Electron microscope carbon-coated copper grids (SPI Supplies, West Chester, PA), Quantifoil R2/1 200 mesh holely-carbon copper grids (Quantifoil Micro Tools, Jena, Germany).
4. Filter paper type #1: 90 mm diameter (Whatman, Clifton, NJ).
5. DUMONT biology anti-capillary reverse tweezers (Ted Pella, Redding, CA).
6. All other reagents except those listed below are from Sigma (St. Louis, MO) and are of analytical grade or higher.

7. Pre-cast 4–12 % SDS-PAGE, 4× SDS sample buffer, and 20× running buffer (Invitrogen, Carlsbad, CA), Amicon concentrators (Millipore, Billerica, MA). Luria-Bertani media (Bacto, NJ).
8. 5 nm Ni-NTA-Nanogold® gold beads from Nanoprobes (Yaphank, NY).
9. Polyethylenimine (Polysciences, PA).
10. pENT-TOPO vectors (Invitrogen).
11. Baculodirect C-term (Invitrogen).

2.3 Buffer Systems

1. Lysis buffer: 25 mM sodium phosphate, pH 7.0, 0 mM NaCl.

2.3.1 CA Purification and Assembly Buffer

2. Hi-Trap QP column buffer: 25 mM sodium phosphate, pH 7.0, 1 mM DTT, and 0.02 % sodium azide, 0 mM NaCl (Low Salt)—1,500 mM NaCl (High Salt).
3. Hi-Trap SP column buffer: 25 mM sodium phosphate, pH 5.8, 1 mM DTT, and 0.02 % sodium azide, 0 mM NaCl (Low Salt)—1,000 mM NaCl (High Salt).
4. Hi-Load Superdex 75 26/60 column buffer: 25 mM sodium phosphate, pH 5.8, 100 mM NaCl, 1 mM DTT, and 0.02 % sodium azide.
5. CA assembly buffer: 50 mM Tris–HCl, pH 8.0, 1 M NaCl.
6. Dilution buffer: 50 mM Tris–HCl, pH 8.0, 100 mM NaCl.

2.3.2 TRIM5α CC-SPRY Expression and Purification Buffer

1. Lysis buffer: 25 mM sodium phosphate, pH 7.5, 250 mM NaCl, 10 mM beta-mercaptoethanol, 0.1 mM PMSF, inhibitor cocktail (Roche), and 0.02 % sodium azide.
2. Hi-Load Superdex 75 26/60 column buffer: 25 mM sodium phosphate, pH 7.5, 150 mM NaCl, 2 mM DTT, 10 % glycerol, and 0.02 % sodium azide.
3. Hi-Trap QP column buffer: 25 mM Tris–HCl, pH 7.5, 2 mM DTT, 10 % glycerol, and 0.02 % sodium azide, a gradient of 0–1,000 mM NaCl.

2.3.3 TRIM5α CC-SPRY Binding Buffer (Also Stock Buffer)

1. Binding buffer: 10 mM Tris–HCl, pH 7.5, 330 mM NaCl, 1 mM TCEP, 0.02 % azide, 5 % glycerol.

2.3.4 Nano-Gold Labeling Buffer

1. 0.05 μM 5 nm Ni-NTA-Nanogold gold beads, 10 mM imidazole, 866 mM NaCl, 42 mM Tris, pH 8.0, 0.2 mM TCEP, 0.004 % sodium azide, 1.25 % glycerol.

2.3.5 Native Core Isolation Buffer

1. STE buffer: 10 mM Tris–HCl, pH 8.0, 100 mM NaCl, 1 mM EDTA.

2.3.6 Crosslinking Buffer

1. Oxider buffer: 60 μM $CuSO_4$, dissolved in water, and 267 μM 1,10-phenanthroline dissolved in 100 % ethanol in a 1:1 ratio.
2. Quench buffer: 20 mM iodoacetamide and 3.7 mM neocuproine.

3 Methods

3.1 Expression and Purification of HIV-1 CA Proteins

1. Amplify and subclone wild-type full-length CA (Pro1-Leu231) into pET21 using *Nde*I and *Xho*I sites.
2. Express full-length CA in *E. coli*, Rosetta 2 (DE3), cultured in Luria-Bertani media and induce with 0.4 mM IPTG. Culture at 23 °C for 16 h.
3. Lyse cells by sonication in the lysis buffer and clear the cell lysate by ultracentrifugation at 100,000 × *g* for 1 h at 4 °C.
4. Let the supernatant flow through a Hi-Trap QP column equilibrated with the lysis buffer.
5. Collect flow through fractions.
6. Reduce the pH of the sample to 5.8 with diluted acetic acid and reduce conductivity to below 2.5 ms/cm by adding Milli-Q water. Centrifuge the sample at 27,666 × *g* with a SLA-1500 rotor for 1 h at 4 °C.
7. Pass the resulting supernatant through a Hi-Trap SP column and collect peak fractions. CA should elute at ~10 ms/cm.
8. Concentrate the sample to 15–18 ml and pass it through a Hi-Load Superdex 75 26/60 gel-filtration column.
9. Collect peak fractions and concentrate with Amicon concentrators to 10 mg/ml, based on the extinction coefficient at UV 280.
10. Analyze protein samples by SDS-PAGE and stain with Coomassie Blue to assess protein purity.
11. For storage, add 5 % glycerol to the sample. Flash freeze 25 μl aliquots and store them at −80 °C.

3.2 Expression and Purification TRIM5α CC-SPRY

1. Amplify and clone the coiled-coil and SPRY domains of human and rhesus TRIM5α (TRIM5α CC-SPRY; residues 132–493 and 134–497, respectively) into the pENT-TOPO vector (Invitrogen), modified to encode a Strep-tag at the N-terminus and a His_6-tag at the C-terminus of the proteins. The Strep-tag is cleavable with TEV protease.
2. Prepare baculoviruses expressing human and rhesus TRIM5α CC-SPRY using the Baculodirect C-term (Invitrogen) according to the manufacturer's protocols.

3. Infect SF21 insect cells with baculoviruses at an MOI of 2 for 40 h.
4. Harvest cells by centrifugation at 4,000 × *g* for 30 min. Lyse cells by sonication in the lysis buffer containing 25 mM sodium phosphate, pH 7.5, 250 mM NaCl, 10 mM beta-mercaptoethanol, 0.1 mM PMSF, inhibitor cocktail (Roche), and 0.02 % sodium azide.
5. Clear cell lysate by ultracentrifugation at 100,000 × *g* for 1 h at 4 °C.
6. Let the supernatant flow through 5 ml Ni-NTA column. The protein is eluted with the lysis buffer containing 500 mM imidazole. Aggregates should be removed by passage over a Hi-Load Superdex 200 16/60 column (GE Healthcare) in a buffer containing 25 mM sodium phosphate, pH 7.5, 150 mM NaCl, 2 mM DTT, 10 % glycerol, and 0.02 % sodium azide.
7. Collect the fraction containing TRIM5α CC-SPRY and dilute it threefold with a buffer containing 25 mM Tris, pH 7.5, 2 mM DTT, 10 % glycerol, and 0.02 % sodium azide.
8. Pass the fraction through a 5 ml Hi-Trap QP column (GE Healthcare) and elute the proteins using a gradient of 0–1 M NaCl. Alternatively, load the fraction onto a 5 ml StrepTrap-HP column (GE Healthcare) and elute with 2.5 mM desbiotin.
9. Flash freeze 20 μl aliquots and store them at –80 °C.

3.3 In Vitro HIV-1 CA Assembly

1. Add 2× assembly buffer to freshly thawed stock protein to a final CA concentration of 2 mg/ml (*see* **Note 1**).
2. Incubate the mixture at 37 °C for 1 h and mix frequently. At the end of incubation, transfer the sample to ice for further analysis.

3.4 TRIM5α CC-SPRY and CA Assembly Binding Assay

We use a binding assay with SDS-PAGE to quantify the binding ratio of TRIM5α CC-SPRY/CA.

1. Add TRIM5α_{hu}CC-SPRY or TRIM5α_{rh}CC-SPRY aliquots from 4 mg/ml stock solutions to the preassembled CA tubes (*see* **Note 2**).
2. Incubate the reaction mixture on a rocking platform at room temperature for 1 h with gentle mixing at 10 min intervals.
3. At the end of incubation, withdraw 5 μl samples from the reaction mixtures and immediately use these for cryoEM analysis.
4. Collect 6 μl samples from the same reaction mixtures and mix these with 4× LDS loading buffer supplemented with 10 mM DTT for SDS-PAGE analysis (t).
5. Pellet the remaining sample at 20,000 × *g* with an Eppendorf centrifuge 5417R for 15 min.

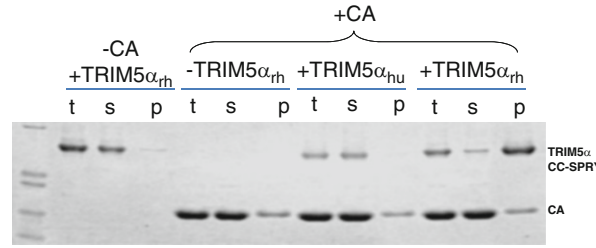

Fig. 1 SDS-PAGE analysis of TRIM5α CC-SPRY binding to CA assemblies. CA tubes were incubated in binding buffer with TRIM5α_{hu} CC-SPRY (10 μM), TRIM5α_{rh} CC-SPRY (18 μM). Samples of the reaction mix before centrifugation (t), of supernatant (s), and of pellet (p) are shown (reproduced from ref. [50], licensed under the Creative Commons Attribution 2.5 Generic License)

6. Collect the supernatants (s) carefully without disturbing the pellets (p)
7. Resuspend the pellet in 1/3 of volume.
8. Mix the supernatant and the resuspended pellet solution with 4× LDS loading buffer.
9. Load the total (t), supernatant (s), and pellet (p) samples, without boiling, onto 10 % SDS-PAGE and stain with Coomassie Blue (Fig. 1).
10. Scan the SDS-PAGE gels and calculate the integrated intensities of CA and TRIM5α_{rh} protein bands in pellet fractions measured using ImageJ 1.40 g program.
11. Calculate the binding molar ratio according to the formula (TRIM5α_{rh} band intensity/TRIM5α_{rh} molecular weight)/(CA band intensity/CA molecular weight).

3.5 CryoEM Specimen Preparation

1. Glow discharge several 200 mesh perforated Quantifoil grids at 25 mA for 25 s.
2. Prepare liquid ethane and wait until it has cooled to near solidifying temperature (*see* **Note 3**).
3. Mount a grid onto an anti-capillary forceps and apply 5 μl sample to the carbon side of the grid (*see* **Note 4**).
4. Mount the forceps onto the plunge-freezing device and make the carbon side face away from you.
5. Quickly blot the excessive solution by pressing filter paper against the bar side for about 6 s.
6. Remove the filter paper and release the plunger at the same time.
7. Transfer the frozen EM grids to storage for later cryoEM analysis.

3.6 CryoEM Study of TRIM5α CC-SPRY Interaction with CA Assemblies

1. Set up a TRIM5α CC-SPRY and CA assembly binding experiment by following the method described in Subheading 3.4.
2. Prepare a cryoEM specimen by following the method described in Subheading 3.5.
3. Load the frozen grid into a Tecnai TF20 microscope.
4. Screen the grid at 120× magnification and find the suitable area with thin ice (*see* **Note 5**).
5. Record all the thin ice areas suitable for imaging in a stage position file.
6. Change the magnification to 50,000× and move to the first position.
7. Switch to diffraction mode; insert and center an objective aperture (*see* **Note 6**).
8. Switch back to imaging mode and lower the magnification to 3,500×.
9. Record a CCD image using a long exposure time of ~1–2 s and a beam spot size of 9 or 10.
10. Identify a thin ice-covered hole with a feature and move the stage to a position in which the feature is at the center of the CCD.
11. Switch to exposure mode and collect a CCD image under low-dose condition (10–15 $e^-/Å^2$).
12. Examine the morphology of the CA assembly after incubating with binding buffer, human and rhesus TRIM5α CC-SPRY (Fig. 2a–c).
13. CryoEM has shown that the structure of tubular CA assembly has been disrupted by rhesus TRIM5α CC-SPRY, resulting in release of linear fragments of CA (Fig. 2c, d).

3.7 Nano-Gold Labeling of TRIM5α CC-SPRY on Capsid Assemblies

It is difficult to visualize the TRIM5α CC-SPRY density on CA tubes in cryoEM micrographs due to low contrast. Since the C-terminus of TRIM5α CC-SPRY is tagged with His_6, we used Ni-NTA nano-gold labeling to confirm its binding to CA assemblies [52]. The method is described in detail here.

1. Assemble the CA tubes as described in Subheading 3.3.
2. Set up both human and rhesus TRIM5α CC-SPRY/CA assembly binding assays, as described in Subheading 3.4.
3. Add 2.7 μl of 5 nm Ni-NTA-Nanogold® gold to the assemblies and incubate the mixture at room temperature for 20 min.
4. Centrifuge the mixture at 3,000 × *g* and resuspend the pellet in assembly buffer.
5. Apply the samples immediately to glow-discharged EM grids for negative staining with 1 % uranyl acetate solution.

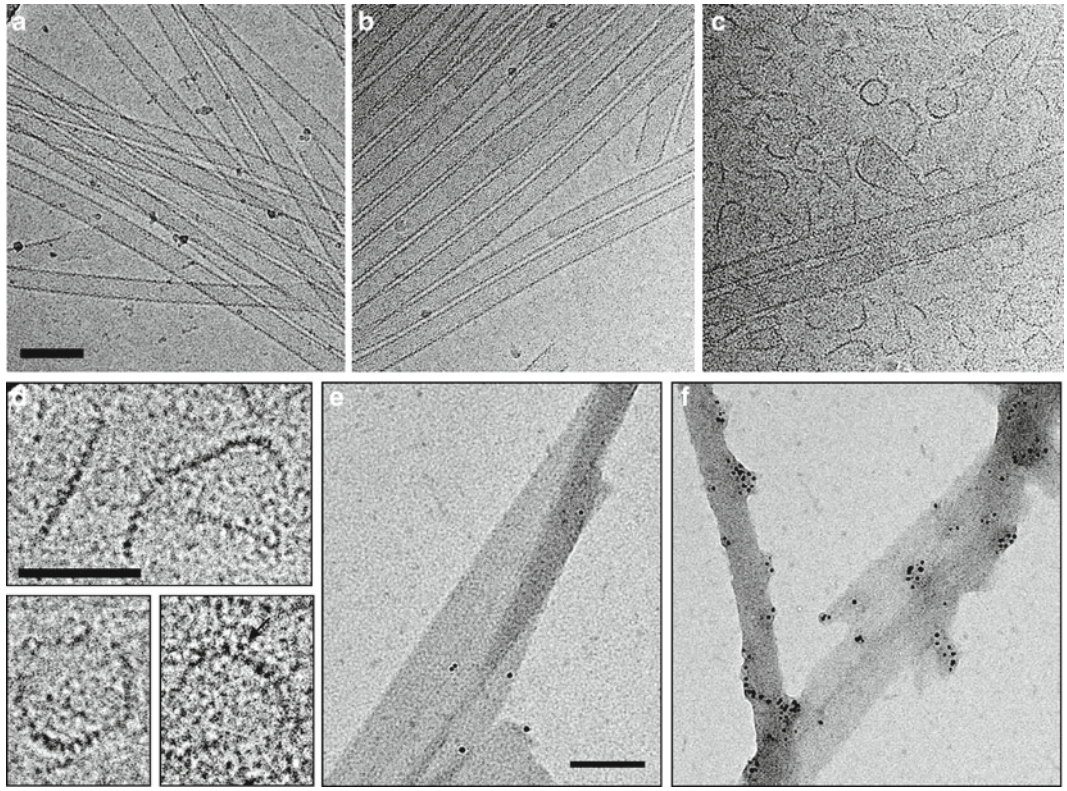

Fig. 2 CryoEM analysis of the TRIM5α CC-SPRY interaction with wild-type CA tubes. (**a**–**c**) Low-dose projection images of CA assemblies (64 μM), incubated with binding buffer (**a**), human (**b**), or rhesus (**c**) TRIM5α CC-SPRY (18 μM). (**d**) Representative assembly fragments, observed after TRIM5α_{rh} CC-SPRY binding. *Arrows* indicate the TRIM5α_{rh} CC-SPRY density. Nano-gold labeling of human (**e**) and rhesus (**f**) TRIM5α CC-SPRY on CA tubes. Scale bars are 100 nm in (**a**–**c**) and (**e** and **f**) and 50 nm in (**d**) (reproduced from ref. [50], licensed under the Creative Commons Attribution 2.5 Generic License)

In rhesus TRIM5α CC-SPRY/CA samples, EM micrographs showed the nano-gold beads clearly decorating the CA tube surfaces (Fig. 2f). In contrast, in human TRIM5α CC-SPRY/CA samples, few gold beads were found to bind to CA tubes (Fig. 2e). These results compliment the previous binding results from SDS-PAGE analysis.

3.8 Inter-Molecular Crosslinking of CA Assemblies

The CA assembly is built with NTD hexameric rings connected by CTD dimers. The hexamers are stabilized by intra-hexamer NTD–NTD and NTD–CTD interactions [15]. The inter-hexamer linkage can be strengthened through a CTD–CTD trimer interface at the local threefold axis [10]. To probe which interface is disrupted by TRIM5α, we used two pair-wise cysteine mutations A14C/E45C, which crosslinks CA into hexamers (Fig. 3a) [15], and P207C/T216C, which crosslinks three CA molecules from neighboring hexamers (Fig. 3b), to stabilize the intra- and inter-hexamer

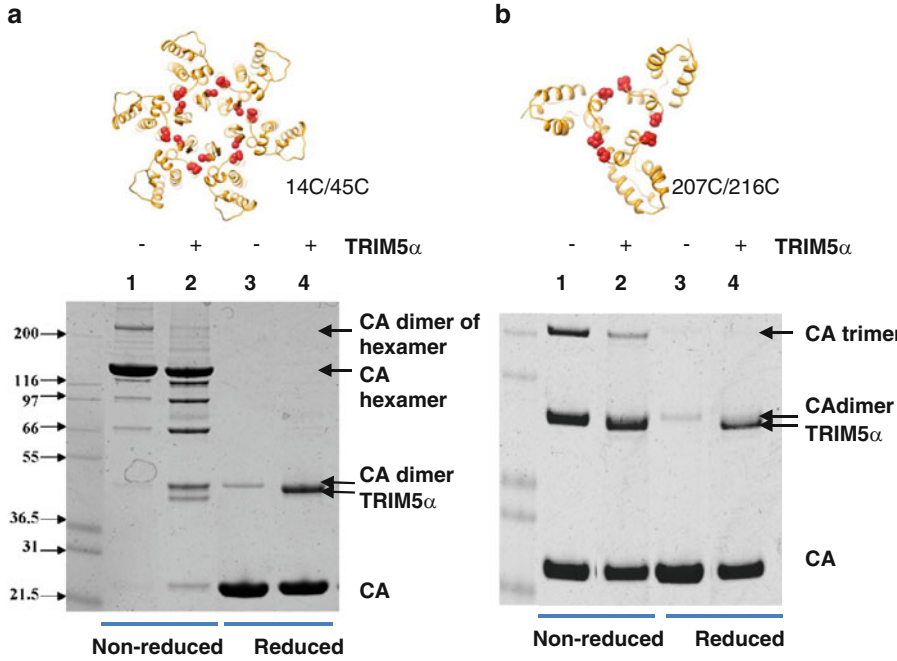

Fig. 3 SDS-PAGE analysis of TRIM5α CC-SPRY interaction with CA assemblies using intra- and inter-hexamer crosslinking. Nonreducing and reducing SDS-PAGE analysis of A14C/E45C CA tubes (**a**) and P207C/T216C CA tubes (**b**) incubated with binding buffer and TRIM5α_{rh} CC-SPRY (18 μM), followed by oxidation. The gel is subjected to Coomassie Blue staining. At the top of panel (**a**) and (**b**), pseudo-atomic model of hexameric NTD ring (pdb code: 1gwp) and CTD trimer (pdb code: 2kod) are shown, respectively. Residuals A14/E45 and P207/T216 are highlighted by *red spheres* (reproduced from ref. [50], licensed under the Creative Commons Attribution 2.5 Generic License)

interfaces, respectively. Incubation of TRIM5α_{rh} CC-SPRY with crosslinked CA assemblies and examining the structural effect using cryoEM provided insight into which interface is more susceptible to TRIM5α disruption [50].

1. Assemble 30 μl P207C/T216C or A14C/E45C CA in the presence of 50 μM DTT under the conditions described in Subheading 3.3.
2. Incubate assembled tubes with binding buffer and TRIM5α_{rh} CC-SPRY (18 μM), as described in Subheading 3.4.
3. Pellet both samples by centrifugation at 20,000 × *g*, at room temperature, in an Eppendorf centrifuge 5417R for 15 min.
4. Resuspend the pellet in 30 μl assembling buffer and oxidize it with 1 μl of 30× oxidizer mix for 5 s.
5. Quench the resuspended pellet solution immediately with 20 mM iodoacetamide and 3.7 mM neocuproine.

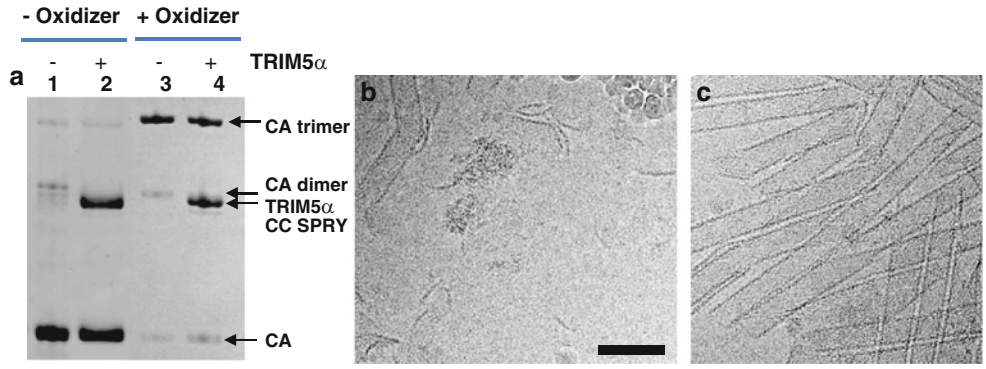

Fig. 4 Inter-hexamer crosslinking prevents CA structural disruption by TRIM5α_{rh} CC-SPRY. (**a**) Nonreducing SDS-PAGE analysis of TRIM5α_{rh} CC-SPRY (18 μM) binding to crosslinked P207C/T216C CA tubes, visualized by Coomassie Blue staining. (**b**, **c**) CryoEM analysis of the structural effect of TRIM5α_{rh} CC-SPRY binding to P207C/T216C CA tubes without (**b**, corresponding sample in panel **a**, lane 2) and with (**c**, corresponding sample in panel **a**, lane 4) crosslinking. Scale bar, 100 nm (reproduced from ref. [50], licensed under the Creative Commons Attribution 2.5 Generic License)

6. Mixed quenched pellet solution with 4× LDS loading buffer.
7. Load the sample, without boiling, on 10 % SDS-PAGE and stain with Coomassie Blue.
8. Our SDS-PAGE analysis confirmed that CA A14C/E45C is crosslinked into hexamers and that CA P207C/T216C is crosslinked into trimers (Fig. 3a lane 1, b lane 1). When incubated with TRIM5α_{rh} CC-SPRY followed by oxidation, the trimer band (Fig. 3b lane 2) was reduced dramatically, whereas the hexamer band (Fig. 3a lane 2) exhibited only a minor reduction, if anything; instead, the dimer of hexamer band was almost completely diminished. These results suggest that TRIM5α disrupts the CA lattice at inter-hexamer interfaces.
9. Incubate TRIM5α_{rh} CC-SPRY with both non-crosslinked (Fig. 4a lane 2) and crosslinked (Fig. 4a lane 4) P207C/T216C mutant CA assembly as described in Subheading 3.4.
10. Analyze the interaction using method described in Subheading 3.6.
11. Previous CryoEM studies have shown that non-crosslinked P207C/T216 mutant CA tubes are susceptible to TRIM5α disruption (Fig. 4b), while the crosslinked assembly is resistant to such structural damage (Fig. 4c).

3.9 Isolation of Crosslinked HIV-1 Cores

We also examined the structural effect of TRIM5α CC-SPRY on native cores. HIV-1 cores with cysteine mutations A14C/E45C and P207C/T216C were isolated using a modified "spin-thru" method previously reported [53].

1. Transiently transfect sixty dishes of 6×10^6 293 T cells with 10 μg plasmid DNA (using 10 μg of HIV-1 construct R9, R9.Env-, or R9.A14C/E45C, or R9.P207C/T216C) using polyethylenimine (3.6 μg/ml, Polysciences) in each 10 cm dish.
2. Collect virus-containing supernatants after 48 h and clarify supernatant by filtration (0.45 μm pore-size).
3. Pellet clarified supernatant (600 ml) through 3 ml cushions of 20 % sucrose (120,000 × *g*, 2.5 h) in a Beckman SW32Ti rotor then gently suspended in a total of 1.2 ml STE buffer for 2 h at 4 °C.
4. Subject the concentrated virus suspension to equilibrium ultracentrifugation (120,000 × *g*, 16 h, 4 °C, Beckman SW-32Ti rotor) through a layer of 1 % Triton X-100 into a linear gradient of 30–70 % sucrose in STE buffer. Collect 1-ml fractions.
5. Determine the CA concentrations using p24 ELISA.
6. Collect the peak p24 fractions near the bottom of the gradient and concentrate to ~100 μl by diafiltration with an Ultracel-10 K protein concentrator.
7. Use nonreducing SDS-PAGE analysis to confirm that both A14C/E45C cores and P207C/T216C cores are spontaneously crosslinked into hexamers and trimers, respectively.

3.10 CryoEM Study of TRIM5α CC-SPRY Interaction with Native HIV-1 Cores

1. Add rhesus or human TRIM5α CC-SPRY proteins to a solution of isolated HIV-1 A14C/E45C or P207C/T216C cores (~11 μg/ml) so that the final CC-SPRY concentration is about 18 μM.
2. Incubate the mixture at room temperature for 1 h on a rocking bed.
3. Prepare cryoEM specimen using the method described in Subheading 3.5.
4. Load the grid into a Tecnai TF20 microscope.
5. Randomly collect 80 low-dose projection images of each sample at 19,000× magnification, under which the field of view covers about 5 μm^2 surface areas (Fig. 5a, b, d, and e).
6. Quantify the number of cores in each sample using average number of cores per image frame.
7. Plot mean value of cores per image with one standard deviation for error bar (Fig. 5c, f).

Our results showed that TRIM5α_{rh} CC-SPRY disrupts A14C/E45C crosslinked cores. On the other hand, inter-hexamer crosslinking (P207C/T216C mutations) rendered the cores resistant to disruptive effect of TRIM5α_{rh} CC-SPRY [50].

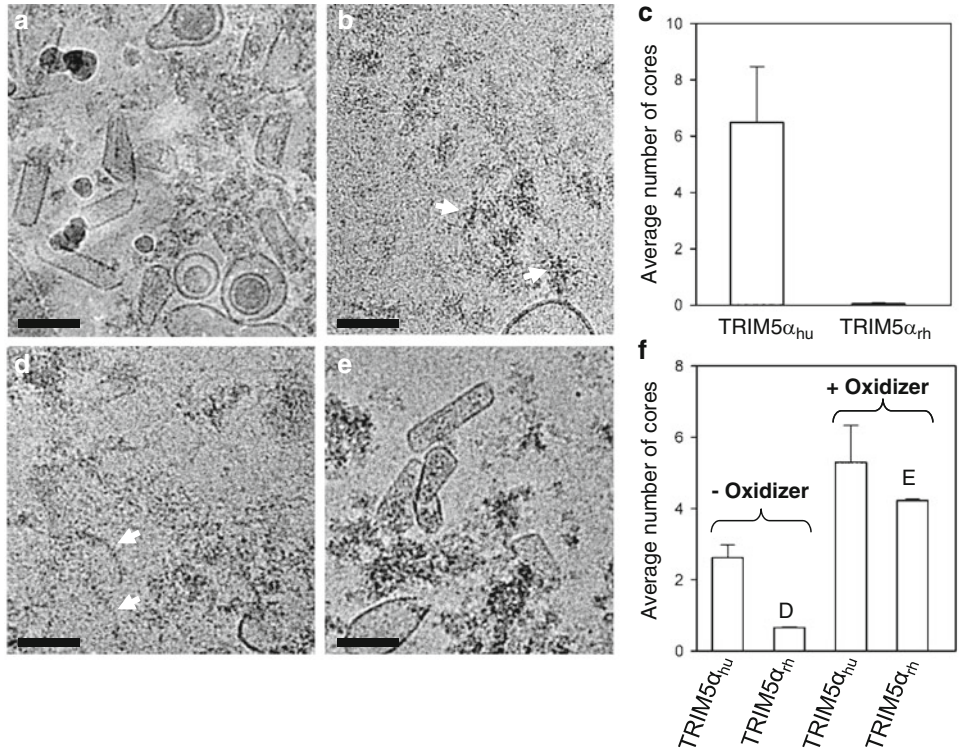

Fig. 5 Structural effects of TRIM5α CC-SPRY$_{rh}$ on isolated HIV-1 cores. (**a**, **b**) Low-dose projection images of purified mutant A14C/E45C cores (11 μg/ml) incubated with human (**a**) or rhesus (**b**) TRIM5α CC-SPRY (18 μM). Scale bar, 100 nm. (**c**) Quantification of the number of cores on the cryoEM grids. The mean values of the average number of cores per image are plotted, with the error bars representing one standard deviation. (**d**, **e**) Representative low-dose projection images of purified P207C/T216C cores, incubated with rhesus TRIM5α CC-SPRY (18 μM), without (**d**) and with (**e**) oxidation for crosslinking. Scale bars, 100 nm. (**f**) Quantification of the number of cores on the cryoEM micrographs (reproduced from ref. [50], licensed under the Creative Commons Attribution 2.5 Generic License)

4 Notes

1. For the CA assembly assay, the sequence of mixing reaction components has an impact on the final number of assembled tubes. The most efficient assembly is achieved by adding 2× assembly buffer to the CA protein stock solution followed by the addition of Milli-Q water.
2. Before carrying out binding experiments, freshly thawed TRIM5α CC-SPRY solution should be spun at 20,000 × *g* for 1 min at 4 °C to remove aggregates, thus minimizing the errors in the binding ratio measurements.
3. Ice contamination is a normal problem during the cryoEM grid preparation. One common source of contamination is contaminated liquid ethane. Ethane should be completely

cooled to near solidifying temperature and kept minimally exposed to air to avoid frost. Also, the remaining ethane gas at the bottom of the tank is not suitable for sample preparation.

4. The CA tubes are assembled at 1 M NaCl. The salt increases the background noise of cryoEM images considerably. For imaging, a drop (3–5 μl) of dilution buffer can be added to the bar side of the grid, and, then, a filter paper can be used to quickly blot away excess solution from the bar side. Due to the quick exchange between sample solution and dilution buffer, structural effects on the sample can be kept to a minimum.
5. Before collecting cryoEM micrographs, it is important to select the areas with the most suitable ice thickness. The data collected at thinner ice areas will normally give a better contrast. It is convenient and time-saving to screen the whole grid first at 120× magnification to find thin ice areas. The thin ice area should show uniform contrast indicating the ice thickness is uniform. Furthermore, the holes should be clearly visible as thicker ice will reduce the contrast from holes on carbon film.
6. Due to the low contrast of frozen-hydrated biological specimens, an objective aperture can be used to enhance the contrast, albeit at the cost of resolution. The objective aperture can also reduce charging problems. Insert and carefully center the objective aperture. Due to potential residual contamination and slight misalignment, the objective stigmatism needs to be readjusted.

Acknowledgments

The authors would like to thank Dr. Jinwoo Ahn and Danxia Ke for technical support, and Dr. Teresa Brosenitsch for critical reading of the manuscript. This work was supported by GM082251 and GM085043.

References

1. Ganser BK, Li S, Klishko VY, Finch JT, Sundquist WI (1999) Assembly and analysis of conical models for the HIV-1 core. Science 283:80–83
2. Gitti RK, Lee BM, Walker J, Summers MF, Yoo S, Sundquist WI (1996) Structure of the amino-terminal core domain of the HIV-1 capsid protein. Science 273:231–235
3. Gamble TR, Vajdos FF, Yoo S, Worthylake DK, Houseweart M, Sundquist WI, Hill CP (1996) Crystal structure of human cyclophilin A bound to the amino-terminal domain of HIV-1 capsid. Cell 87:1285–1294
4. Gamble TR, Yoo S, Vajdos FF, von Schwedler UK, Worthylake DK, Wang H, McCutcheon JP, Sundquist WI, Hill CP (1997) Structure of the carboxyl-terminal dimerization domain of the HIV-1 capsid protein. Science 278: 849–853
5. Kelly BN, Howard BR, Wang H, Robinson H, Sundquist WI, Hill CP (2006) Implications for viral capsid assembly from crystal structures of HIV-1 Gag(1-278) and CA(N)(133-278). Biochemistry 45:11257–11266
6. Momany C, Kovari LC, Prongay AJ, Keller W, Gitti RK, Lee BM, Gorbalenya AE, Tong L,

McClure J, Ehrlich LS, Summers MF, Carter C, Rossmann MG (1996) Crystal structure of dimeric HIV-1 capsid protein. Nat Struct Biol 3:763–770
7. Worthylake DK, Wang H, Yoo S, Sundquist WI, Hill CP (1999) Structures of the HIV-1 capsid protein dimerization domain at 2.6 A resolution. Acta Crystallogr D Biol Crystallogr 55:85–92
8. Ternois F, Sticht J, Duquerroy S, Krausslich HG, Rey FA (2005) The HIV-1 capsid protein C-terminal domain in complex with a virus assembly inhibitor. Nat Struct Mol Biol 12:678–682
9. Ivanov D, Tsodikov OV, Kasanov J, Ellenberger T, Wagner G, Collins T (2007) Domain-swapped dimerization of the HIV-1 capsid C-terminal domain. Proc Natl Acad Sci U S A 104:4353–4358
10. Byeon IJ, Meng X, Jung J, Zhao G, Yang R, Ahn J, Shi J, Concel J, Aiken C, Zhang P, Gronenborn AM (2009) Structural convergence between Cryo-EM and NMR reveals intersubunit interactions critical for HIV-1 capsid function. Cell 139:780–790
11. Berthet-Colominas C, Monaco S, Novelli A, Sibai G, Mallet F, Cusack S (1999) Head-to-tail dimers and interdomain flexibility revealed by the crystal structure of HIV-1 capsid protein (p24) complexed with a monoclonal antibody Fab. EMBO J 18:1124–1136
12. Du S, Betts L, Yang R, Shi H, Concel J, Ahn J, Aiken C, Zhang P, Yeh JI (2011) Structure of the HIV-1 full-length capsid protein in a conformationally trapped unassembled state induced by small-molecule binding. J Mol Biol 406:371–386
13. Li S, Hill CP, Sundquist WI, Finch JT (2000) Image reconstructions of helical assemblies of the HIV-1 CA protein. Nature 407:409–413
14. Ganser-Pornillos BK, Cheng A, Yeager M (2007) Structure of full-length HIV-1 CA: a model for the mature capsid lattice. Cell 131:70–79
15. Pornillos O, Ganser-Pornillos BK, Kelly BN, Hua Y, Whitby FG, Stout CD, Sundquist WI, Hill CP, Yeager M (2009) X-ray structures of the hexameric building block of the HIV capsid. Cell 137:1282–1292
16. Pornillos O, Ganser-Pornillos BK, Banumathi S, Hua Y, Yeager M (2010) Disulfide bond stabilization of the hexameric capsomer of human immunodeficiency virus. J Mol Biol 401: 985–995
17. Pornillos O, Ganser-Pornillos BK, Yeager M (2011) Atomic-level modelling of the HIV capsid. Nature 469:424–427
18. Aiken C (2006) Viral and cellular factors regulating HIV-1 uncoating. Curr Opin HIV AIDS 1:194–199
19. Arhel N (2010) Revisiting HIV-1 uncoating. Retrovirology 7:96
20. Best S, Le Tissier P, Towers G, Stoye JP (1996) Positional cloning of the mouse retrovirus restriction gene Fv1. Nature 382:826–829
21. Stremlau M, Owens CM, Perron MJ, Kiessling M, Autissier P, Sodroski J (2004) The cytoplasmic body component TRIM5alpha restricts HIV-1 infection in Old World monkeys. Nature 427:848–853
22. Sayah DM, Sokolskaja E, Berthoux L, Luban J (2004) Cyclophilin A retrotransposition into TRIM5 explains owl monkey resistance to HIV-1. Nature 430:569–573
23. Pertel T, Reinhard C, Luban J (2011) Vpx rescues HIV-1 transduction of dendritic cells from the antiviral state established by type 1 interferon. Retrovirology 8:49
24. Yap MW, Nisole S, Lynch C, Stoye JP (2004) Trim5alpha protein restricts both HIV-1 and murine leukemia virus. Proc Natl Acad Sci U S A 101:10786–10791
25. Perez-Caballero D, Hatziioannou T, Yang A, Cowan S, Bieniasz PD (2005) Human tripartite motif 5 alpha domains responsible for retrovirus restriction activity and specificity. J Virol 79:8969–8978
26. Sawyer SL, Wu LI, Emerman M, Malik HS (2005) Positive selection of primate TRIM5alpha identifies a critical species-specific retroviral restriction domain (see comment). Proc Natl Acad Sci U S A 102:2832–2837
27. Song B, Javanbakht H, Perron M, Park DH, Stremlau M, Sodroski J (2005) Retrovirus restriction by TRIM5alpha variants from Old World and New World primates. J Virol 79:3930–3937
28. Stremlau M, Perron M, Lee M, Li Y, Song B, Javanbakht H, Diaz-Griffero F, Anderson DJ, Sundquist WI, Sodroski J (2006) Specific recognition and accelerated uncoating of retroviral capsids by the TRIM5alpha restriction factor. Proc Natl Acad Sci U S A 103: 5514–5519
29. Perron MJ, Stremlau M, Lee M, Javanbakht H, Song B, Sodroski J (2007) The human TRIM5alpha restriction factor mediates accelerated uncoating of the N-tropic murine leukemia virus capsid. J Virol 81:2138–2148
30. Shi J, Aiken C (2006) Saturation of TRIM5 alpha-mediated restriction of HIV-1 infection depends on the stability of the incoming viral capsid. Virology 350:493–500
31. Sebastian S, Luban J (2005) TRIM5alpha selectively binds a restriction-sensitive retroviral capsid. Retrovirology 2:40
32. Pertel T, Hausmann S, Morger D, Zuger S, Guerra J, Lascano J, Reinhard C, Santoni FA, Uchil PD, Chatel L, Bisiaux A, Albert ML, Strambio-De-Castillia C, Mothes W, Pizzato

M, Grutter MG, Luban J (2011) TRIM5 is an innate immune sensor for the retrovirus capsid lattice. Nature 472:361–365
33. Reymond A, Meroni G, Fantozzi A, Merla G, Cairo S, Luzi L, Riganelli D, Zanaria E, Messali S, Cainarca S, Guffanti A, Minucci S, Pelicci PG, Ballabio A (2001) The tripartite motif family identifies cell compartments. EMBO J 20:2140–2151
34. Nisole S, Stoye JP, Saib A (2005) Trim family proteins: retroviral restriction and antiviral defence. Nat Rev Microbiol 3:799–808
35. Ozato K, Shin DM, Chang TH, Morse HC 3rd (2008) TRIM family proteins and their emerging roles in innate immunity. Nat Rev Immunol 8:849–860
36. Aravind L, Koonin EV (2000) The U box is a modified RING finger—a common domain in ubiquitination. Curr Biol 10:R132–R134
37. Freemont PS (2000) RING for destruction? Curr Biol 10:R84–R87
38. Lienlaf M, Hayashi F, Di Nunzio F, Tochio N, Kigawa T, Yokoyama S, Diaz-Griffero F (2011) Contribution of E3-ubiquitin ligase activity to HIV-1 restriction by TRIM5{alpha} rh: structure of the RING domain of TRIM5{alpha}. J Virol 85(17):8725–8737
39. Mische CC, Javanbakht H, Song B, Diaz-Griffero F, Stremlau M, Strack B, Si Z, Sodroski J (2005) Retroviral restriction factor TRIM5alpha is a trimer. J Virol 79: 14446–14450
40. Javanbakht H, Yuan W, Yeung DF, Song B, Diaz-Griffero F, Li Y, Li X, Stremlau M, Sodroski J (2006) Characterization of TRIM5alpha trimerization and its contribution to human immunodeficiency virus capsid binding. Virology 353:234–246
41. Maillard PV, Ecco G, Ortiz M, Trono D (2010) The specificity of TRIM5{alpha}-mediated restriction is influenced by its coiled-coil domain. J Virol 84(11):5790–5801
42. Li X, Sodroski J (2008) The TRIM5{alpha} B-box 2 domain promotes cooperative binding to the retroviral capsid by mediating higher-order self-association. J Virol 82(23): 11495–11502
43. Diaz-Griffero F, Qin XR, Hayashi F, Kigawa T, Finzi A, Sarnak Z, Lienlaf M, Yokoyama S, Sodroski J (2009) A B-box 2 surface patch important for TRIM5 alpha self-association, capsid binding avidity, and retrovirus restriction. J Virol 83:10737–10751
44. Stremlau M, Perron M, Welikala S, Sodroski J (2005) Species-specific variation in the B30.2(SPRY) domain of TRIM5 alpha determines the potency of human immunodeficiency virus restriction. J Virol 79: 3139–3145
45. Yap MW, Nisole S, Stoye JP (2005) A single amino acid change in the SPRY domain of human Trim5 alpha leads to HIV-1 restriction. Curr Biol 15:73–78
46. Ohkura S, Yap MW, Sheldon T, Stoye JP (2006) All three variable regions of the TRIM5alpha B30.2 domain can contribute to the specificity of retrovirus restriction. J Virol 80:8554–8565
47. Song B, Gold B, O'Huigin C, Javanbakht H, Li X, Stremlau M, Winkler C, Dean M, Sodroski J (2005) The B30.2(SPRY) domain of the retroviral restriction factor TRIM5alpha exhibits lineage-specific length and sequence variation in primates. J Virol 79:6111–6121
48. James LC, Keeble AH, Khan Z, Rhodes DA, Trowsdale J (2007) Structural basis for PRYSPRY-mediated tripartite motif (TRIM) protein function. Proc Natl Acad Sci U S A 104:6200–6205
49. Ganser-Pornillos BK, Chandrasekaran V, Pornillos O, Sodroski JG, Sundquist WI, Yeager M (2010) Hexagonal assembly of a restricting TRIM5alpha protein. Proc Natl Acad Sci U S A 108:534–539
50. Zhao G, Ke D, Vu T, Ahn J, Shah VB, Yang R, Aiken C, Charlton LM, Gronenborn AM, Zhang P (2011) Rhesus TRIM5alpha disrupts the HIV-1 capsid at the inter-hexamer interfaces. PLoS Pathog 7:e1002009
51. Erickson-Viitanen S, Manfredi J, Viitanen P, Tribe DE, Tritch R, Hutchison CA 3rd, Loeb DD, Swanstrom R (1989) Cleavage of HIV-1 gag polyprotein synthesized in vitro: sequential cleavage by the viral protease. AIDS Res Hum Retroviruses 5:577–591
52. Reddy V, Lymar E, Hu M, Hainfeld JF (2005) 5 nm gold-Ni-NTA binds His tags. Microsc Microanal 11:1118–1119
53. Aiken C (2009) Cell-free assays for HIV-1 uncoating. Methods Mol Biol 485:41–53

http://www.springer.com/978-1-62703-669-6

Human Retroviruses
Methods and Protocols
Vicenzi, E.; Poli, G. (Eds.)
2014, XVIII, 345 p. 62 illus., 38 illus. in color., Hardcover
ISBN: 978-1-62703-669-6
A product of Humana Press